

## The effect of the chemical composition of a ferrallitic soil on neutron probe calibration

C. Grimaldi<sup>a,\*</sup>, M. Grimaldi<sup>b</sup>, M. Vauclin<sup>c</sup>

<sup>a</sup>*Institut National de la Recherche Agronomique, Science du Sol, 78026 Versailles Cedex, France*

<sup>b</sup>*ORSTOM, 213 Rue La Fayette, 75480 Paris Cedex 10, France*

<sup>c</sup>*Laboratoire d'étude des Transferts en Hydrologie et Environnement, CNRS-1512, INPG, UJF, BP53, 38041 Grenoble Cedex 9, France*

### Abstract

In a ferrallitic soil in French Guiana, the neutron probe calibration appeared to be problematic: considerable variations in the neutron count rate were observed at very short range and with an almost constant volumetric water content. This local variability of the count rate was explained by the mineralogical heterogeneity of the schist weathering horizon where subvertically oriented layers are especially rich in boron, element with large thermal neutron absorption cross section. Various calibration methods were carried out and their limits were pointed out. The field gravimetric calibration without taking into account the soil physical and chemical spatial variations appeared to be risky, even if different pedological horizons are considered separately. A calibration based on the neutron absorption  $\Sigma_a$  and diffusion  $\Sigma_d$  cross sections calculated from chemical analysis led to overestimates of the volumetric water content. This could be explained by the concentration of boron atoms in sand-size tourmaline crystals which reduces their neutron absorption properties. The direct measurement of thermal neutron absorption and diffusion cross sections on soil samples in a graphite pile seems to be the best calibration procedure, but it has to be repeated as often as the spatial variability required.

*Keywords:* Neutron probe calibration; Ferrallitic soil; Tourmaline; Boron

### 1. Introduction

The impact of deforestation on water balances was studied in French Guiana on the ECEREX facility, consisting of ten small watersheds (Roche, 1982; Fritsch, 1992). In order to study water transfers in relation to the pedological cover (Boulet et al., 1982; Guehl, 1984; Grimaldi and Boulet, 1990), tensiometers and neutron access tubes were set up on

\* Corresponding author.

some of the watersheds. During this study, the neutron probe proved to be particularly difficult to use. In fact, within a few decimeters of one another and with an almost constant water content, considerable variations in the neutron count rate were recorded.

A neutron probe consists of a “fast” neutron source and a detector measuring thermal neutron flux, i.e. “slowed down” by the soil and re-emitted towards the probe. In the interaction of neutrons with the soil, the hydrogen of water plays an essential role because of its neutron slowing down and scattering properties (McHenry, 1963). Assaying water with a neutron probe is therefore based on the relationship between the thermal neutron count rate and the water content of the soil volume influencing the measurement. However, the atoms in the solid phase also have an effect on neutrons (Holmes, 1966; Couchat, 1967, 1974). The constitutional hydrogen apparently has the same effect as the hydrogen of free water (Marais and Smit, 1962). Certain atoms have a large thermal neutron absorption cross section, thus reducing the flux reaching the detector: chlorine (Olgaard, 1965), manganese, iron (Burn, 1966) and especially trace elements such as boron (Holmes and Jenkinson, 1959; Olgaard, 1965) and gadolinium (Nicolls et al., 1977). Among the physical parameters, the effect of soil density is frequently studied because this parameter determines the volumetric concentration of the different atoms which act on neutrons (Marais and Smit, 1962; Waters and Moss, 1966; Luebs et al., 1968; Lal, 1974; Greacen and Schrale, 1976). The spatial distribution of the different atoms must also be taken into account as is shown in experiments which vary the amount and size distribution of the gravel fraction (Lal, 1979; Babalola, 1978).

Consequently, neutron probe calibration is an essential step on which the accuracy of water content estimates greatly depends (Sinclair and Williams, 1979; Haverkamp et al., 1984; Vauclin et al., 1984; Bertuzzi et al., 1987). The most usual method is the field gravimetric calibration method (Rawls and Asmussen, 1973; Vachaud et al., 1977), which involves determining a regression line between the neutron count rate and volumetric water content. The same procedure is sometimes used in the laboratory with the soil reconstituted in drums (Hugues and Forrest, 1971), which requires some means of controlling its density. A completely different method developed by Couchat et al. (1975) calculates a calibration line by introducing thermal neutron absorption and scattering characteristics of the dry soil in a mathematical model. These characteristics are either measured directly on a soil sample or calculated using soil chemical analyses. All these methods require that the soil volume to which the calibration relation is applied be homogeneous with respect to the interactions of the neutrons with the solid phase.

In a tropical environment, the limits of assaying water with the neutron probe have been stressed by Lal (1974, 1979) and more recently by Ruprecht and Schofield (1990) for particularly heterogeneous lateritic soils. The aim of this article is to identify the soil characteristics influencing the neutron count rate on the site and, considering their spatial variability, to discuss the interest and limits of different calibration methods.

## **2. Materials and Methods**

### *2.1. The site*

The experimental site was on the “B” watershed of the ECEREX facility (Sarrailh, 1990) in French Guiana, in the North East of the South American continent (5°15'N and

53°W). The watershed is in a tropical rainforest. The annual rainfall varies from 2500 to 4000 mm, with a dry season from September to November when the monthly rainfall is often below 50 mm. The geological substratum is the Bonidoro Precambrian schist, which is very fine micaschist, rich in muscovite and quartz, and visible below a depth of 20 m.

## 2.2. The soil

The pedological profile (Grimaldi et al., 1992) shows under a thin humic horizon, a set of yellowish brown horizons, ranging from clayey sand to sandy clay, rich in ferruginous nodules and quartz sand, and macroporous (from 0.05 to 0.6 m). Through a strong-brown and clayey transition horizon with sinuous boundaries (from 0.6 to 0.7 or 1 m), the soil changed to a red, compact, clayey horizon, rich in fine loam of partially kaolinized muscovite particles (Tandy et al., 1990). Throughout the profile, the clay fraction was made up of kaolinite intercrystallized with iron oxyhydroxides: hematite in the red horizon and goethite in the horizons above.

## 2.3. Equipment

We used a Solo 25 neutron probe and a CPN 501B gamma density probe, made by Nardeux (France) and Campbell Pacific Nuclear (USA), respectively. The neutron moisture meter had a  $^3\text{He}$  detector and a mid-placed Am-Be source of 1480 MBq activity. The gamma density probe contained a  $^{137}\text{Cs}$  source of 370 MBq activity and a Geiger Müller detector, located at 5.4 and 27 cm of the probe bottom, respectively. The neutron access tube was in aluminium, with an inside diameter of 41 mm and an outside diameter of 45 mm. The counting time was 21 s for the neutron probe and 60 s for the gamma density probe. The average count rates in the soil (2 replications) were divided by the average count rates (10 replications), in the water for the neutron probe and for the gamma density probe on its container as recommended by the manufacturer. The measurements in a standard environment were taken before and after the measurements in the soil. The neutron and gamma photon ratios are labelled  $n$  and  $d$ , respectively.

We took into consideration the conclusions of Valles et al. (1989) who showed that the centre of measurement of the gamma density probe differed by 0.11 m compared with the indications provided by the constructor. Moreover, in order to take into account the unusually high electronic density of hydrogen compared to the other atoms, we followed the advice of Christensen (1974) and introduced a term correcting for the water content, to estimate the wet density of the soil using gamma photon count rates. Thus, if  $\theta$  is the volumetric water content of the soil ( $\text{m}^3 \cdot \text{m}^{-3}$ ),  $\rho_w$  the density of the water ( $\text{kg} \cdot \text{m}^{-3}$ ) and  $\rho_h$  the correct wet density of the soil ( $\text{kg} \cdot \text{m}^{-3}$ ), the estimated wet density is given by:

$$\rho'_h = \rho_h + 0.11 \cdot \rho_w \cdot \theta \quad (1)$$

The calibration line equation of the gamma probe, established on the experimental site, was:

$$\rho'_h = 3.017 - 0.555 \cdot d \quad (2)$$

The coefficients of this calibration line, as well as their variances and covariance, have

been calculated with unbiased estimators proposed by Bertuzzi et al. (1987). The standard deviation of the prediction error was 0.030 for  $\rho'_h = 2 \text{ kg} \cdot \text{m}^{-3}$ .

#### 2.4. Measurements

A neutron access tube, labelled A, was installed in the soil after boring 1.90 m deep with an auger. The tube went successively through the yellowish brown nodular horizons from 0.1 to 0.6 m, the strong-brown clay horizon from 0.6 to 0.9 m and the red clay horizon from 0.9 m down. Ten other holes, labelled B to K, were bored over a period of three months (November to January) during which the water status of the soil naturally varied. These bore-holes were distributed around tube A on a circular surface area of 1.5 m diameter, at least 0.4 m apart. The gravimetric water content  $W$  ( $\text{kg} \cdot \text{kg}^{-1}$ ) of the samples taken in 0.10 m increments were measured in the laboratory, after they were oven-dried at  $105^\circ\text{C}$  for 48 hours. A tube was inserted in each new bore-hole in order to carry out neutron counts between a depth of 0.25 and 1.75 m, every 0.1 m, and the same day in tube A. Gamma photon counts were also recorded at the same depths. Thus the dry bulk density  $\rho_d$  ( $\text{kg} \cdot \text{m}^{-3}$ ) and the volumetric water content  $\theta$  of the samples taken in each bore-hole were calculated by:

$$\text{as } \rho_d = \rho_h - \rho_w \cdot \theta \quad (3)$$

$$\text{and } \theta = W \cdot \rho_d / \rho_w \quad (4)$$

$$\text{according to Eqs. (1) and (3), } \rho_d = \rho'_h - 1.11 \cdot \rho_w \cdot \theta \quad (5)$$

$$\text{according to Eqs. (4) and (5), } \rho_d = \rho'_h - 1.11 \cdot \rho_d \cdot W = \rho'_h / (1 + 1.11 \cdot W) \quad (6)$$

$$\text{and } \theta = W \cdot \rho'_h / (1 + 1.11 \cdot W) \cdot \rho_w \quad (7)$$

#### 2.5. Soil constitution analysis and study of soil chemical composition influence on neutron count

On all of the samples taken in the 11 bore-holes, A to K, the  $1000^\circ\text{C}$  mass loss was measured and the major elements (silicon, aluminium, iron, calcium, magnesium, sodium, potassium) were analysed by atomic absorption after being dissolved in three acids (hydrochloric, sulfuric and nitric acids). The residue left by this treatment, essentially made up of quartz grains ( $\text{SiO}_2$ ), was also quantified. We calculated a multiple linear regression model in which the neutron count ratio was explained by the volumetric water and chemical element contents:

$$n = a_0 + a_1 \cdot \theta + \sum a_i \cdot [X_i] \quad (8)$$

where  $a_0$ ,  $a_1$ ,  $a_i$ : constants and  $[X_i]$ : volumetric concentration of element  $X_i$ . Using a "backward selection" method, we chose a limited number of variables, which were not correlated with each other, to obtain a more simple model with in particular optimum accuracy for the volumetric water content coefficient.

At location A, each 0.10 m portion of the material extracted was dissolved in hydrofluoric and perchloric acids for more detailed chemical analysis. Silicium, aluminium and titanium

were estimated using X-ray fluorescence; iron, calcium, magnesium, sodium, potassium, lithium, manganese using atomic absorption. Boron was determined by IPC (Inductive Plasma Coupling) after alkaline fusion with metaphosphate. From these chemical analyses, the total absorption ( $\Sigma a$ ) and diffusion ( $\Sigma d$ ) cross sections were calculated for each depth of tube A, using the following formula:

$$\Sigma a = N_0 \cdot \Sigma_i (m_i \cdot \sigma a_i / A_i) \text{ and } \Sigma d = N_0 \cdot \Sigma_i (m_i \cdot \sigma d_i / A_i) \quad (9)$$

where  $\Sigma a$  and  $\Sigma d$ : total absorption and diffusion cross sections ( $\text{cm}^2 \cdot \text{g}^{-1}$ )

$N_0$ : Avogadro's constant =  $6.02 \cdot 10^{23}$

$m_i$ : massic content ( $\text{g} \cdot \text{g}^{-1}$ ) of element  $i$

$\sigma a_i$  and  $\sigma d_i$ : absorption and diffusion atomic cross sections ( $\text{cm}^2$ ) of element  $i$  (Mughabghab et al., 1981)

$A_i$ : atomic mass (g) of element  $i$

On some samples,  $\Sigma a$  and  $\Sigma d$  were direct measured at the CEA in Cadarache (France): the disturbance of the thermal neutron flux in a graphite pile was recorded when dry soil samples (300 g) were introduced (Couchat et al., 1975).

## 2.6. Neutron probe calibration

According to the gravimetric calibration (Vachaud et al., 1977), the volumetric water content measurements carried out in the eleven bore-holes, A to K, were expressed according to the count ratios  $n_A$  obtained the same day at the same depth for tube A. The calibration relations are written:

$$\theta = a + b \cdot n_A \quad (10)$$

where  $a$  and  $b$  are constants.

The multiple linear regression model (8), in which  $n$  was explained by  $\theta$  and the more significant chemical variables, was also used as calibration relation.

Finally, given a ( $\Sigma a$ ,  $\Sigma d$ ) couple, either calculated from chemical analyses or directly measured in a graphic pile, the model established by the CEA makes it possible to calculate the coefficients  $\alpha$ ,  $\beta$ ,  $\gamma$  and  $\delta$  of the calibration line (Couchat, 1974; Couchat et al., 1975):

$$n = (\alpha \cdot \rho_d + \beta) \cdot \theta + \gamma \cdot \rho_d + \delta \quad (11)$$

## 3. Results and Discussion

### 3.1. Neutron count and soil constitution vertical and lateral variability

The measurements carried out when tube A was installed clearly showed the difficulty in calibrating the neutron probe in this type of soil. Between 0.75 and 1.75 m in depth, the neutron count ratio decreased considerably, from 0.55 to 0.34, whereas the volumetric water content remained almost constant, approximately  $0.40 \text{ m}^3 \cdot \text{m}^{-3}$  (Fig. 1a). The eleven bore-holes on the site showed considerable variability in the neutron count ratio profiles. The

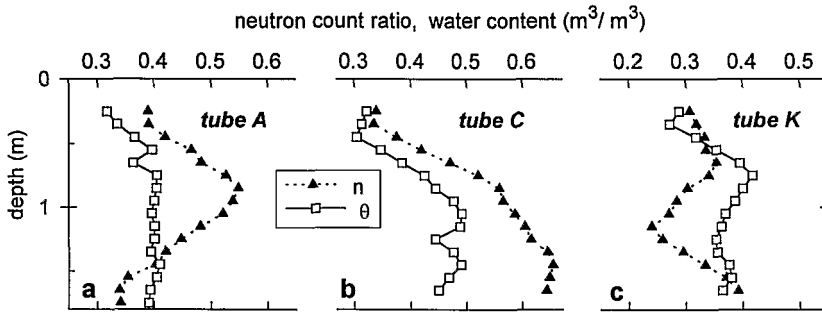


Fig. 1. Neutron count ratio and volumetric water content profiles measured when tube A (a), tube C (b) and tube K (c) were installed.

variability was not only due to a spatial or temporal variation of the water status of the soil. For example, in the red horizon of bore-holes A, C and K (Fig. 1), the neutron count ratio was either increasing or decreasing, whereas the volumetric water content variations with depth were small. The neutron count rate must therefore depend on vertical and lateral variations of one or several other soil characteristics.

Fig. 2 illustrates the local spatial variability of the soil for some physical and chemical characteristics, on a surface area of 2 m<sup>2</sup>. The iron content in particular varied as much vertically as laterally. We can relate this to a variable concentration of nodules in the upper horizons and to a variable thickness of the strong-brown clayey horizon, the least rich in iron and the least dense. The concentrations of potassium, localized in muscovite, illustrate the mineralogical heterogeneity of the parent rock. This heterogeneity is no more visible to the naked eye in the strongly weathered red horizon.

### 3.2. Influence of chemical composition of soil on the neutron count

A multiple linear regression model appeared satisfactory for explaining the neutron count ratios based on the volumetric water, iron and magnesium contents:

$$n = 1.212 \cdot \theta - 0.366 \cdot 10^{-3} \cdot [\text{Fe}] - 0.1540 \cdot [\text{Mg}] + 0.145 \quad (12)$$

$$(\pm 0.052) \quad (\pm 0.033 \cdot 10^{-3}) \quad (\pm 0.0070) \quad (\pm 0.022)$$

with  $r^2 = 0.875$ , and residual standard deviation = 0.033, for 161 observations, where [Fe] and [Mg] are the volumetric iron and magnesium contents (kg · m<sup>-3</sup>). The values between brackets under each of the coefficients correspond to their respective standard deviations. The negative coefficients correspond to neutron absorption. The influence of iron atoms on the absorption of thermal neutrons (Burn, 1966) was confirmed by this regression model. It was surprising to see magnesium appear here, since it was not very abundant in the soil studied (Table 1) and its neutron absorption and diffusion properties are particularly low (Mughabghab et al., 1981). Magnesium was in fact associated with boron in the brown to green dravite, a variety of tourmaline recognized with X-rays on the location, with the formula  $\text{Al}_6\text{Mg}_3\text{Na}(\text{Si}_6\text{O}_{18})(\text{BO}_3)_3(\text{OH},\text{F})_4$ . The correlation between magnesium and boron analysed on bore-hole A samples was distinct in the red horizon (Fig. 3). The

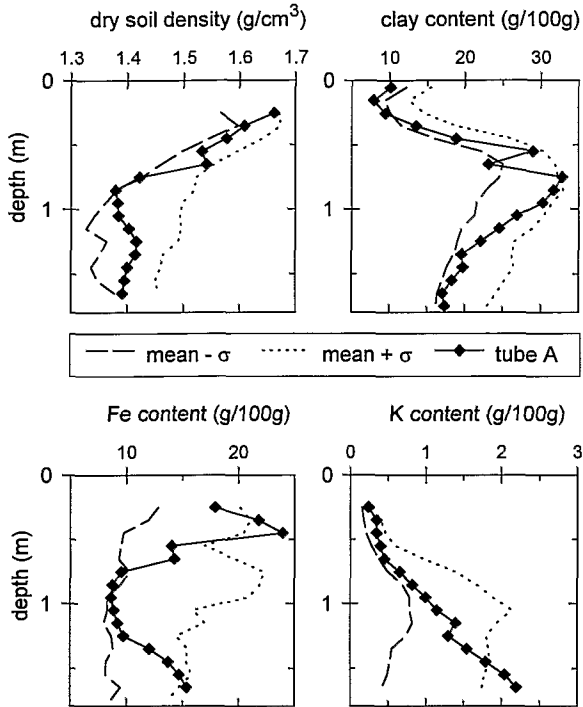


Fig. 2. Local variability of the soil constitution: dry soil density, clay, iron and potassium contents. Comparison between bore-hole A and mean profile  $\pm$  standard deviation of the 11 bore-holes A to K.

influence of boron thus appeared indirectly in the multiple linear regression model (12) through magnesium.

The influence of iron and boron atoms on the absorption of thermal neutrons (Fig. 4) was calculated at each depth based on the bore-hole A chemical analyses (Table 1) and using the Eq. (9). In comparison, the other atoms, hydrogen, silicon, titanium, aluminium and, deep down, potassium and lithium contributed more moderately.  $\Sigma a$  was relatively high between 0.2 and 0.6 m, i.e. in the nodular horizons where the iron was concentrated and the boron content was significant together. Then from 0.8 m down,  $\Sigma a$  increased progressively with the boron content. The diffusion of neutrons was especially due to hydrogen and oxygen (Fig. 4). Their concentrations in the dry soil were estimated using the 1000°C mass loss and oxides associated to the different elements ( $\text{SiO}_2$ ,  $\text{Al}_2\text{O}_3$ , etc...).  $\Sigma d$  varied little throughout the profile, but increased slightly between 0.4 and 1 m, in the most clayey layers.

The multiple linear regression model on all the eleven bore-holes and the calculation of  $\Sigma a$  and  $\Sigma d$  on the bore-hole A showed that the variability of the neutron count ratio profiles could be explained by the vertical and lateral variability of the iron and above all boron content, matching that of magnesium. Thus for all bore-holes, and in particular for bore-holes A, C and K chosen above, the lowest neutron count ratios (Fig. 1) corresponded to

Table 1  
Chemical composition of bore-hole A samples

Depth (m)	1000°C mass loss	Si (g/100 g)	Al (g/100 g)	Fe (g/100 g)	Ti (g/100 g)	K (g/100 g)	Na (g/100 g)	Ca (g/100 g)	Mg (g/kg)	B (g/kg)	Mn (g/kg)	Li (g/kg)
0–0.1	7.86	35.60	2.72	5.21	0.51	0.19	0.03	0.14	0.23	0.20	0.09	0.01
0.1–0.2	6.72	26.80	3.63	19.05	0.39	0.23	0.03	0.03	0.26	0.16	0.06	0.01
0.2–0.3	6.93	27.60	3.73	17.10	0.39	0.22	0.03	0.03	0.26	0.16	0.06	0.01
0.3–0.4	7.05	20.70	5.36	24.50	0.59	0.40	0.05	0.03	0.35	0.19	0.07	0.01
0.4–0.5	7.78	19.90	7.44	22.95	0.71	0.54	0.06	0.03	0.36	0.15	0.08	0.02
0.5–0.6	8.48	25.80	8.95	10.15	0.73	0.53	0.06	0.03	0.41	0.15	0.08	0.02
0.6–0.7	8.63	27.40	9.63	7.85	0.78	0.72	0.08	0.03	0.38	0.11	0.08	0.02
0.7–0.8	8.56	26.30	9.84	7.71	0.84	0.79	0.09	0.03	0.43	0.09	0.09	0.02
0.8–0.9	8.53	24.30	12.30	8.90	1.05	1.16	0.12	0.03	0.58	0.13	0.10	0.03
0.9–1.0	8.37	23.80	13.45	9.00	0.99	1.37	0.14	0.03	0.60	0.14	0.11	0.04
1.0–1.1	7.90	23.10	13.53	9.65	1.12	1.70	0.17	0.03	0.72	0.19	0.13	0.04
1.1–1.2	7.44	22.20	13.03	10.10	1.16	1.89	0.19	0.03	0.76	0.22	0.13	0.04
1.2–1.3	7.33	22.60	12.70	11.85	1.14	2.02	0.21	0.03	0.85	0.27	0.13	0.04
1.3–1.4	7.30	20.30	12.65	14.40	1.16	2.16	0.22	0.03	0.90	0.30	0.13	0.04
1.4–1.5	7.14	20.80	13.24	13.40	1.26	2.48	0.26	0.03	1.00	0.39	0.15	0.05
1.5–1.6	7.25	20.40	12.99	13.55	1.27	2.67	0.28	0.03	1.00	0.38	0.14	0.05
1.6–1.7	6.95	20.30	13.16	13.10	1.24	2.58	0.26	0.03	0.99	0.45	0.14	0.05
1.7–1.8	6.98	20.70	12.98	13.15	1.22	2.40	0.25	0.03	1.00	0.39	0.15	0.05
1.8–1.9	6.77	19.90	13.16	14.25	1.19	2.56	0.26	0.03	0.92	0.45	0.15	0.05

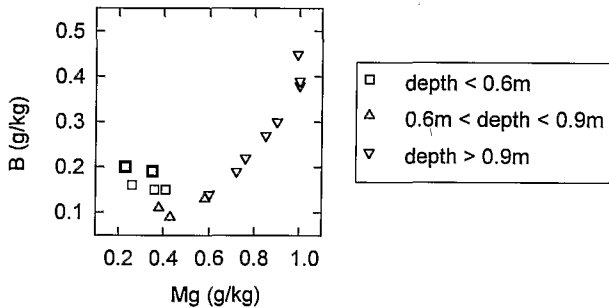


Fig. 3. Boron content versus magnesium content for bore-hole A.

the highest magnesium contents which appeared at variable depths (Fig. 5). Tourmaline distribution heterogeneity is related to the presence of soil layers rich in residual minerals with a conserved original subvertical dip of the schist. Thus two neighbouring bore-holes cross these boron-rich volumes at different depths.

### 3.3. Comparison of neutron probe calibration methods

The volumetric water contents measured on the samples of the eleven bore-holes A to K were expressed according to the count ratios obtained the same day at the same depth for tube A. We separated two sets of measurements corresponding to:

– nodular horizons and strong-brown clayey horizon, down to a depth of 0.9 m (Fig. 6a);



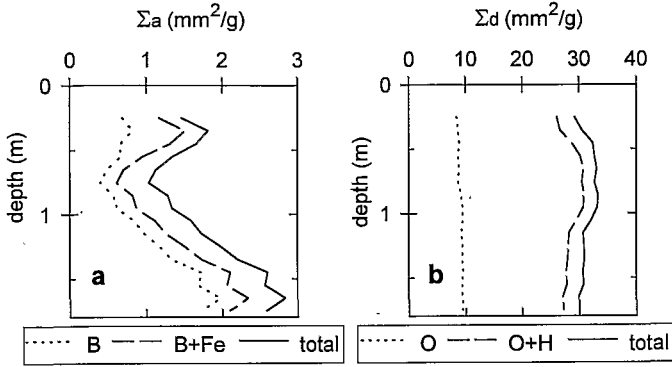


Fig. 4. Thermal neutron absorption cross-section ( $\Sigma a$ ) profiles (bore-hole A) for boron, boron plus iron, and all elements (a). Thermal neutron diffusion cross-section ( $\Sigma d$ ) profiles (bore-hole A) for oxygen, oxygen plus hydrogen, and all elements (b).

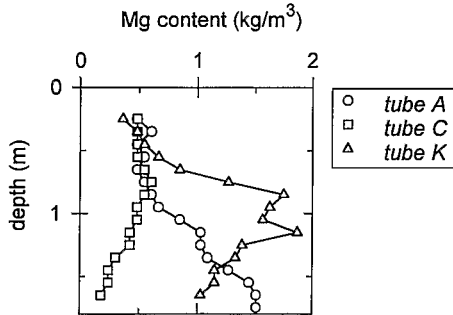


Fig. 5. Magnesium content profile for bore-holes A, C and K.

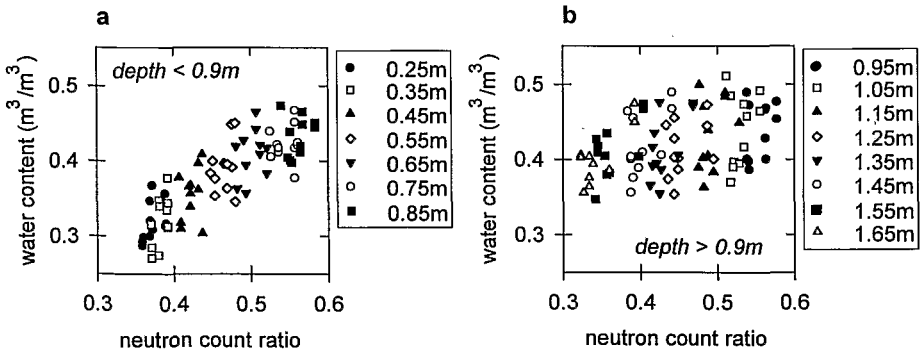


Fig. 6. Volumetric water content versus neutron count ratio for the nodular and strong-brown clayey horizons (a), and for the red clay horizon (b). Experimental values obtained at each depth are identified by various symbols.

– red clay horizon, below a depth of 0.9 m (Fig. 6b).

On each of these graphs, the full set of measurements forms a roughly elongated cluster. We tested a linear regression model (10) for the different soil depth groups studied. The correlation coefficient was maximum for the soil layer between 0.2 and 0.9 m deep and mediocre for the regression carried out on the 0.9–1.8 m layer (Table 2). The measurements taken at each depth, represented by different symbols, form however sub-groups of points which only partially overlap. On the 0.2–0.9 m layer, the systematic increase in volumetric water content with depth can no doubt be explained by the increase in clay content (Fig. 2). However, it is recognized that clay content also influences the neutron count, independently of water content, because of mineral constitutive hydrogen atoms. It was therefore risky to retain a single calibration line for the first two horizons because this would admit that the variations in clay content and chemical composition did not influence the calibration line coefficients. In the red horizon, variations of chemical constitution, in particular of boron, clearly influence the relation between  $\theta$  and  $n$ . On both graphs the sub-groups of points corresponding to each depth had a distinctly different orientation from the main axis of the cluster (Fig. 6).

The multiple linear regression model and the CEA model took into account the influence of soil constitution on the calibration line. The intercept of the calibration line varied with iron and magnesium contents in the Eq. (12). The slope and the intercept of the calibration line, calculated using the CEA model (11), varied at each depth because of  $\Sigma a$  and  $\Sigma d$  variations. Table 3 groups together the coefficients of the calibration lines, of the form:  $\theta = a + b \cdot n$ , obtained for tube A using Eqs. (11) and (12). Their reliability was assessed by calculating the volumetric water contents corresponding to the neutron count ratios obtained when tube A was set up and by comparing them with the measured water contents (Fig. 7). With the multiple linear regression model, the volumetric water content was overestimated for tube A. The difference between  $\theta$  measured and  $\theta$  calculated reached  $0.05 \text{ m}^3 \cdot \text{m}^{-3}$  (Fig. 7). The comparison of calculated and measured humidity profiles for tube C and K (Fig. 8) confirmed however the pertinence of variables explaining the neutron count ratio. For each of the tubes, the coefficients of the model (12) were recalculated by removing the measurements and analyses carried out on this tube. The RMSEP (root mean squared error of prediction) of  $\theta$  was  $0.027 \text{ (m}^3 \cdot \text{m}^{-3})$  for all the tubes. In comparison, the accuracy of the estimation of volumetric water content by field gravimetric calibration for more homogeneous soils varies between 0.01 (Haverkamp et al., 1984) and 0.02 (Bertuzzi

Table 2

Coefficients and estimated variances and covariances of the field gravimetric calibration lines of the neutron probe for selected soil layers

Depth (m)	$a$ (*)	$b$ (*)	$s^2(a)$	$s^2(b)$	$s^2(a,b)$	$s^2(e)$	$r$	No. observations
0.2–0.6	0.0225	0.793	$0.218 \cdot 10^{-2}$	$0.129 \cdot 10^{-1}$	$-0.529 \cdot 10^{-2}$	$0.578 \cdot 10^{-3}$	0.824	47
0.6–0.9	0.2165	0.383	$0.790 \cdot 10^{-2}$	$0.273 \cdot 10^{-1}$	$-0.147 \cdot 10^{-1}$	$0.477 \cdot 10^{-3}$	0.659	33
0.2–0.9	0.0959	0.611	$0.446 \cdot 10^{-3}$	$0.204 \cdot 10^{-2}$	$-0.943 \cdot 10^{-3}$	$0.567 \cdot 10^{-3}$	0.892	80
0.9–1.7	0.3283	0.212	$0.694 \cdot 10^{-3}$	$0.340 \cdot 10^{-2}$	$-0.152 \cdot 10^{-2}$	$0.135 \cdot 10^{-2}$	0.506	87

\*  $\theta = a + bn_A$ .

Table 3

Calibration lines coefficients obtained for tube A with: the multiple linear regression model (Eq. 12) and the CEA model (Eq. 11) based on soil total chemical analyses or on direct measurement of  $\Sigma a$  and  $\Sigma d$

Depth (m)	Chemical analysis, and multiple linear regression (12)		Chemical analysis, calculation of $\Sigma a$ and $\Sigma d$ , and CEA model (11)		Direct measurement of $\Sigma a$ and $\Sigma d$ and CEA model (11)	
	<i>b</i> (*)	<i>a</i> (*)	<i>b</i> (*)	<i>a</i> (*)	<i>b</i> (*)	<i>a</i> (*)
0.25	0.825	0.031	1.133	-0.083		
0.35	0.825	0.063	1.277	-0.082		
0.45	0.825	0.056	1.211	-0.085		
0.55	0.825	0.014	1.075	-0.083		
0.65	0.825	0.008	0.980	-0.088	0.924	-0.104
0.75	0.825	-0.010	0.951	-0.075	0.929	-0.089
0.85	0.825	-0.007	1.050	-0.069	0.886	-0.073
0.95	0.825	0.001	1.076	-0.069	0.886	-0.073
1.05	0.825	0.025	1.182	-0.064	0.911	-0.065
1.15	0.825	0.050	1.239	-0.063		
1.25	0.825	0.052	1.340	-0.065		
1.35	0.825	0.070	1.437	-0.066		
1.45	0.825	0.099	1.603	-0.066		
1.55	0.825	0.126	1.528	-0.066		
1.65	0.825	0.136	1.715	-0.065		
1.75	0.825	0.130	0.592	-0.062		

\*  $\theta = a + bn$ .

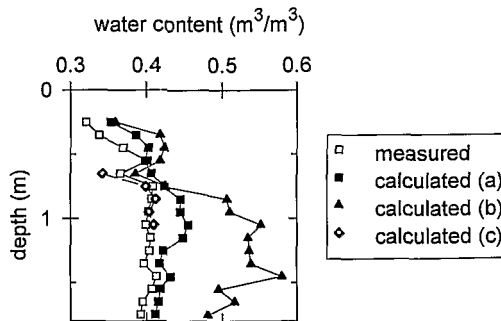


Fig. 7. Comparison between  $\theta$  measured when tube A was installed and  $\theta$  calculated with: (a) the multiple linear regression model (Eq. 12), (b) the CEA model (Eq. 11) based on soil total chemical analyses and (c) the CEA model (Eq. 11) based on direct measurement of  $\Sigma a$  and  $\Sigma d$ .

et al., 1987). When the total absorption and diffusion cross sections were calculated based on the chemical analyses, the volumetric water contents calculated by the CEA model were strongly overestimated, especially in the red horizon (Fig. 7). The boron concentration in the tourmaline crystals, which appears as fine sand (50 to 200  $\mu\text{m}$ ) could explain this discrepancy. In fact, for a similar chemical composition soil sample,  $\Sigma a$  directly measured

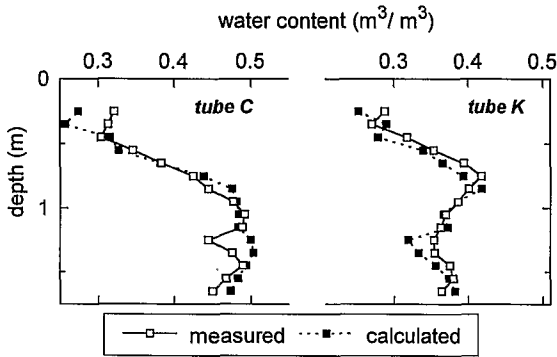


Fig. 8. Comparison between  $\theta$  measured when tubes C and K were installed and  $\theta$  calculated with the multiple linear regression model (Eq. 12).

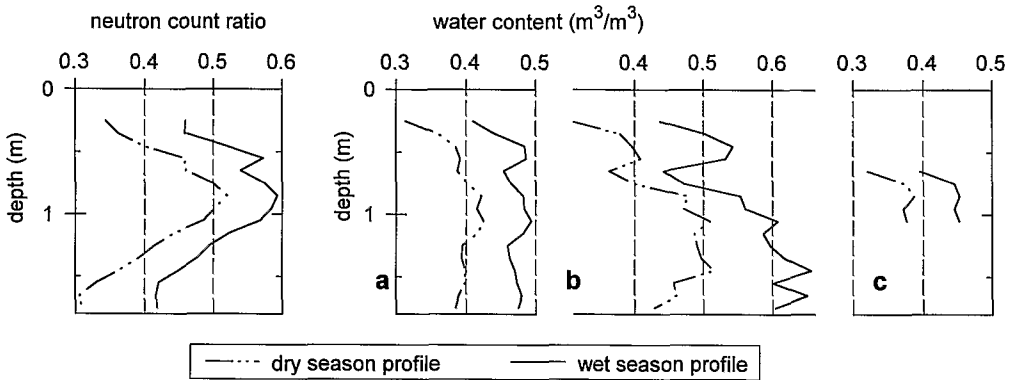


Fig. 9. Seasonal variations of the neutron count ratio profile for tube A and corresponding volumetric water content profiles calculated with: (a) the multiple linear regression model (Eq. 12), (b) the CEA model (Eq. 11) based on soil total chemical analyses and (c) the CEA model (Eq. 11) based on direct measurement of  $\Sigma a$  and  $\Sigma d$ .

was two times lower than  $\Sigma a$  calculated with the chemical analyses when the boron atoms distribution was assumed uniform in the soil. This comparison was done for the soil layer between 0.6 and 1.1 m (Fig. 7). Thus, the CEA model with  $\Sigma a$  and  $\Sigma d$  direct measurements provided the best estimation of the water content.

The slope of the calibration line was dependent on the calibration procedure (Table 3) and had consequences on the estimation of seasonal variations of water content profile (Fig. 9).

#### 4. Conclusion

On the ECEREX watersheds in French Guiana, determining the water content with a neutron probe rapidly appeared to be problematic, since the spatial variability of the neutron

count rate was large and mainly independent of the water content. This study has made it possible to identify the main soil constituents involved: iron in various forms depending on the pedological horizons and at very variable concentrations, and especially tourmaline containing boron, distributed heterogeneously particularly in the weathered red clayey horizon of the schist. Boron has a higher thermal neutron absorption capacity than iron, which was however much more abundant. The distinct vertical differentiation of the soil, associated with the pedogenesis, as well as the mineralogical heterogeneity of the schist and its subvertical structure were responsible for the considerable local variability of the neutron count rate.

A field gravimetric calibration of the neutron probe was therefore hazardous even if the different pedological horizons were considered separately. We took advantage of the soil variability to establish a linear regression model where the neutron count rate was explained by the volumetric water, iron and magnesium contents, magnesium being associated with boron in tourmaline. This model was proposed as calibration relation which requires only routine analyses. The constant slope of the calibration line restricts the interest of this model for water balances calculations. The slope and intercept of calibration lines determined with the CEA model based on the chemical composition of the soil were different at each depth, showing the extent of the variations in the thermal neutron absorption cross section. However, calculating the absorption and diffusion cross sections of the dry soil assumed a uniform distribution of boron and iron atoms in the solid matrix. Their concentration in sand-size tourmaline crystals and in ferruginous nodules, respectively, reduced greatly their neutron absorption effect. This explained the overestimates of the volumetric water content calculated in this way. The direct measurement of these cross sections was certainly more reliable, but these relatively costly measurements have to be repeated as often as the spatial variability required.

### Acknowledgements

This work was supported by ORSTOM and was partly conducted in the framework of the programme: “Influence à l’échelle régionale des couvertures pédologiques et végétales sur les bilans hydriques et minéraux des sols” funded by CNRS/PIREN, INRA, ORSTOM & CIRAD. The authors wish to thank R. Guennelon (INRA) for encouragement and advice along this study, P. Moutonnet (CEA Cadarache) for use the CEA model, J. Delvigne (ORSTOM) for X-rays identification of the dravite, C. Durier (INRA Versailles) for advice on statistical calculation and C. Young (INRA Jouy-en-Josas) for translation of this paper.

### References

- Babalola, O., 1978. Field calibration and use of the neutron moisture meter on some nigerian soils. *Soil Sci.*, 126: 118–124.
- Bertuzzi, P., Bruckler, L. and Gros, C., 1987. Régression linéaire avec erreur sur les variables: application à l’étalonnage d’un gammadensimètre à transmission et d’un humidimètre à neutrons. *Agronomie* 7: 507–515.
- Boulet, R., Humbel, F.X. and Lucas, Y., 1982. Analyse structurale et cartographie en pédologie. III - Passage de la phase analytique à une cartographie générale synthétique. *Cah. ORSTOM, sér. Pédologie*, XIX: 341–351.

- Burn, K.N., 1966. Effect of iron on measuring water content with a neutron meter. *Nature*, 210: 763–764.
- Christensen, E.R., 1974. Use of the gamma density gauge in combination with the neutron moisture probe. In: *Isotope and Radiation Techniques in Soil Physics and Irrigation Studies*. International Atomic Energy Agency, Vienna, IAEA-SM-176-1.
- Couchat, P., 1967. Détermination de la courbe d'étalonnage de l'humidimètre à neutrons  $\alpha$  partir de l'analyse chimique des sols. In: *Isotopes and Radiation Techniques in Soil Physics and Irrigation Studies*. FAO/IAEA Symp. Istanbul, 67–82.
- Couchat, P., 1974. Mesure neutronique de l'humidité des sols. Thesis, Univ. Toulouse, France.
- Couchat, P., Carre, C., Marcesse, J. and Le Ho, J., 1975. The measurement of thermal neutron constants of the soil: Application to the calibration of neutron moisture gauges and to the pedological study of soil. Proc. Conf. Nuclear Data Cross Sections on Technology, Washington, D.C.
- Fritsch, J.M., 1992. Les effets du défrichement de la forêt amazonienne et de la mise en culture sur l'hydrologie de petits bassins versants. Opération ECEREX en Guyane française. ORSTOM (Ed.), coll. Etudes et Thèses, Paris.
- Graecen, E.L. and Schrale, G., 1976. The effect of bulk density on neutron meter calibration. *Aust. J. Soil Res.*, 14: 159–169.
- Grimaldi, M. and Boulet, R., 1990. Relation entre l'espace poral et le fonctionnement hydrodynamique d'une couverture pédologique sur socle de Guyane française. *Cah. ORSTOM, sér. Pédologie*, XXV: 263–275.
- Grimaldi, C., Grimaldi, M. and Boulet, R., 1992. Etude d'un système de transformation sur schiste en Guyane française. Approches morphologique, géochimique et hydrodynamique. In: Wackermann, J.M.: *Organisation et fonctionnement des altérites et des sols*. ORSTOM (Ed.), coll. Colloques et Séminaires, Paris, 81–98.
- Guehl, J.M., 1984. Dynamique de l'eau dans le sol en forêt tropicale humide guyanaise. Influence de la couverture pédologique. *Ann. Sci. For.*, 41: 195–236.
- Haverkamp, R., Vauclin, M. and Vachaud, G., 1984. Error analysis in estimating soil water content from neutron probe measurements: I. Local standpoint. *Soil Sci.*, 137: 78–90.
- Holmes, J.W., 1966. Influence of bulk density of soil on the neutron moisture meter calibration. *Soil Sci.*, 102: 355–360.
- Holmes, J.W. and Jenkinson, A.F., 1959. Techniques for using the neutron moisture meter calibration. *J. Agr. Eng. Res.*, 4: 100–109.
- Hughes, M.W. and Forrest, J.A., 1971. Laboratory calibration of the neutron moisture meter. CSIRO Aust. Div. of Soils, Notes on Soil Techniques, 32–37.
- Lal, R., 1974. The effect of soil texture and density on the neutron and density probe calibration for some tropical soils. *Soil Sci.*, 117: 183–190.
- Lal, R., 1979. Concentration and size of gravel in relation to neutron moisture and density probe calibration. *Soil Sci.*, 127: 41–50.
- Luebs, R.E., Brown, M.J. and Laag, A.E., 1968. Determining water content of different soils by the neutron method. *Soil Sci.*, 106: 207–212.
- McHenry, J.R., 1963. Theory and application of neutron scattering in the measurement of soil moisture. *Soil Sci.*, 95: 294–307.
- Marais, P.G. and Smit, W.B. de V., 1962. Effect of bulk density and of hydrogen in forms other than free water on the calibration curve of the neutron moisture meter. *South African J. Agr. Sci.*, 5: 225–238.
- Mughabghab, S.F., Divadeenam, M., Holden, N.E., 1981. *Neutron Cross Sections*. Vol. 1, part A. Academic Press, New York.
- Nicolls, K.D., Hutton, J.T. and Honeysett, J.L., 1977. Gadolinium in soils and its effect on the count rate of the neutron moisture meter. *Aust. J. Soil Res.*, 15: 287–291.
- Olgaard, P.L., 1965. On the theory of the neutronic method for measuring the water content in soil. Riso Rep. No. 97, Danish AEC.
- Rawls, W.J. and Asmussen, L.E., 1973. Neutron probe field calibration for soils in the Georgia coastal plain. *Soil Sci.*, 116: 262–265.
- Roche, M.A., 1982. Comportements hydrologiques comparés et érosion de l'écosystème forestier amazonien à ECEREX, en Guyane. *Cah. ORSTOM, sér. Hydrologie*, XIX: 81–114.
- Ruprecht, J.K. and Schofield, N.J., 1990. In situ neutron moisture meter calibration in lateritic soils. *Aust. J. Soil Res.*, 28: 153–165.

- Sarrailh, J.M., 1990. Mise en valeur de l'écosystème forestier guyanais; opération ECEREX. INRA-CTFT (Ed.), coll. *Ecologie et Aménagement de l'espace rural*, Paris.
- Sinclair, D.F. and Williams, J., 1979. Components of variance involved in estimating soil water content change using a neutron moisture meter. *Aust. J. Soil Res.*, 17: 237–247.
- Tandy, J.C., Grimaldi, M., Grimaldi, C. and Tessier, D., 1990. Mineralogical and textural changes in French guiana oxisols and their relation with microaggregation. In: Douglas, L.A.: (Ed.), *Soil Micromorphology*. Elsevier Science Publishers B.V., Amsterdam, 191–198.
- Vachaud, G., Royer, J.M. and Cooper J.D., 1977. Comparison of methods of calibration of a neutron probe by gravimetry or neutron-capture model. *J. Hydrol.*, 34: 343–356.
- Valles, V., Guiresse, M. and Tcherbakov, R., 1989. Vérification de la coïncidence géométrique des points de mesure neutronique et gammamétrique pour Solo 40 et CPN 501B. *Bull. Gr. Fr. Humid. Neutron.*, 9: 55–64.
- Vauclin, M., Haverkamp, R. and Vachaud, G., 1984. Error analysis in estimating soil water content from neutron probe measurements: 2. Spatial standpoint. *Soil Sci.*, 137: 141–148.
- Waters, E.H. and Moss, G.F., 1966. Estimation of moisture content by neutron scattering: Effect of sample density and composition. *Nature*, 209: 287–289.